MECHANICAL AND ACOUSTIC BEHAVIOUR OF POROSITY CONTROLLED BIOCOMPOSITE

Justin Merotte[1,2], Antoine Le Duigou[1], Alain Bourmaud[1], Karim Behlouli[2] and Christophe Baley[1]

[1]Université de Bretagne Sud, IRDL, FRE CNRS 3744, Rue Saint Maudé, 56321 Lorient Cedex, France
[2]EcoTechnilin SAS, ZA Caux Multipôles, RD 6015, 76190 Valliquerville, France

Keywords: Biocomposite, Porosity, Mechanical properties, Acoustic properties, Microstructure

Abstract

Due to their ability to combine in a unique material good mechanical and acoustic properties, commingled plant fibers and polypropylene (PP) nonwovens are attractive to the automotive industry. This double function can be achieved by the presence of a controlled porosity content within the composite material, achieved by monitoring the compaction rate during moulding. This study aims to highlight the necessity of a very large porosity volume fraction (60%) to reach good acoustic properties and helps to understand its consequences on the material mechanical behaviour. By combining tensile testing, acoustic absorption measurement and scanning electron imaging analysis, the microstructure, acoustic and mechanical properties have been investigated and are found to be intimately related to the material porosity content. As expected, when increasing porosity level from 5 to 60%, the material behaviour changes and its tensile properties (modulus, strength) drop drastically. This change of properties and behaviour is due to a modification of the material microstructure involving different failure mechanisms.

1. Introduction

Thanks to their ability to combine acoustic absorption and mechanical properties in a unique product, nonwoven biocomposites are becoming a major asset to the automotive industry, especially in car interior parts. Supported by state regulations [1], the use of materials that minimize automotive fuel consumption and thus environmental burdens have been prioritized. Car manufacturers have increased their interest in plant fibre composites in order to improve the end of life (recycling ability [2]) and environmental impact (weigth saving) of their vehicles.
Among the available plant fibres, flax offers high specific tensile stiffness, which is comparable to glass fibres [3]. Within the different methods used to manufacture nonwoven materials [4], needle punched nonwovens combined with polypropylene (PP) fibers are widely used in the automotive industry due to significant material deformation and reduced cycle times during the moulding process. Bos [5] has highlighted the advantage of using flax fibre nonwovens which has been confirmed by Oksman in a comparative study of commercially available semi-finished natural fibre mat reinforced thermoplastics composites [6]. Mieck et al. [7] investigated the mechanical characterization of needle punched nonwoven flax/PP and demonstrated a strong increase of the tensile properties with the fibre content.
As mentioned previously, acoustic absorption of fibrous materials can be adjusted by varying the compaction rate during moulding [8], [9]. This change of compression modifies the geometry and connections of the pores but also modifies the quantity of dry fibres that oscillate and absorb energy [10]. As underlined by Madsen et al. on flax/PP unidirectional and nonwoven composites moulded by

Excerpt from ISBN 978-3-00-053387-7

a film stacking process [11], [12]; increasing the porosity content (up to 30%) tends to drastically decrease the material stiffness .
This paper investigates the effect on mechanical and acoustic properties of large porosity content in a flax/PP nonwoven composite. Therefore, according to the microstructure induced by the porosity content, the acoustic and tensile properties as well as damage mechanisms will be studied. This knowledge will then help in taking full advantage of the porosity content to develop lighter biocomposite while satisfying mechanical and acoustic requirements.

2. Materials and methods

2.1. Materials

Flax tows (*Linum usitatissimum* L. from the Normandy area of France) were used as reinforcement fibres in the nonwoven combined with polypropylene fibres. The industrial commingled nonwoven was manufactured according to the carding/overlapping/needle punching technology [4] at a fibre matrix ratio of 50%-wt and was provided by EcoTechnilin SAS in France under its commercial name Fibriplast LinPP 300. Its areal weight was 273±16 g/m². Flax and polypropylene (PP) fibres densities were measured according to the immersion method of the ISO 1183-1 standard.

2.2. Composite manufacturing

Commingled nonwoven were hot compression moulded on a LabTec Scientific 50T hydraulic press and 15x15cm plates were obtained. A range of porosity contents from 5 to 70% were obtained by setting the plate thickness to a constant value and stacking different quantities of nonwoven plies into the mould (from 2 to 8 plies). The plies were hot pressed (200°C and 11 bar) at a thickness of 2mm for 3 min. They were then placed between cooled plates (cooling rate of 4°C/s and 27 bar) and pressed for 3mins at a final thickness of 2 mm. Changing the number of plies in the stack change the overall volume of porosity. However, the location as well as the shape and size distribution of porosities is not controlled.

2.3. Porosity content measurement

The porosity content has been determined according to ASTM D2734-09 2009. The weight and volume of the composite were measured and the percentage of porosity was determined using the following equation

$$\Phi = 1 - \rho_c \left(\frac{1-w_f}{\rho_m} + \frac{w_f}{\rho_f} \right) \quad (1)$$

Where Φ is the porosity content, ρ_c, ρ_m, ρ_f the composite, matrix and fibre densities respectively and w_f the fibre weight ratio. For low porosity contents, results have been double checked using image analysis of composite cross sections.

2.4. Acoustic tests

The influence of porosity content on normal incident sound absorption coefficient has been assessed using an impedance tube (44 mm diameter) according to transfer function method ISO 10534-2. 3 samples were tested and the normal absorption coefficient (α) has been measured between 200 Hz and 4.3 kHz. Circular specimens (44.3 mm diameter) were milled from composite plates moulded at a thickness of 5 mm. Composite plies number was adjusted to reach the following porosity contents: 5, 30, 60, 70%. These values have been compared to a flax/PP compound reinforced at a fibre volume fraction of 40%.

2.5. Tensile tests and damage analysis

Excerpt from ISBN 978-3-00-053387-7

Static and cyclic tensile tests were performed to assess static properties and damage. According to ISO-527-2, dog-bone geometry specimens were tested on a MTS Synergie RT/1000 (static load) and Instron 5566A (cyclic load) tensile machines. The capacity of the two load cells was 10 kN and a 25 mm nominal length extensometer was used. At least 5 samples were tested at a crosshead displacement of 1 mm.min^{-1}. For the damage analysis, repeated progressive loadings (RPL) were performed. The first loading cycle represented 5% of the load at yield (during the static test). Each subsequent step was increased by 5% up to 20% of yield load and then by 10% until failure. The initial tensile modulus was calculated in the first cycle. The next moduli corresponded to the slope between the beginning of reloading and the point where the reloading loop meets the previous unloading loop [13]. A damage variable is calculated as follows

$$d = 1 - \frac{E}{E_0} \tag{2}$$

Where E is the modulus calculated for each cycle [13] and E_0 the initial modulus. The microstructure change is evaluated by calculating the slope of the curve d=f($\varepsilon/\varepsilon_r$). Where ε is the cycle unloading deformation and ε_r is the deformation at maximum stress.

2.6. Scanning Electron microscopy

The composite structures were observed by scanning electron microscopy (SEM). The samples were embedded in paraffin wax and cut using a Leica RM2135 microtome. The wax was then diluted using two baths of xylene (5min immersion each), three baths of decreasing alcohol contents (96% for 5 min, 90% for 5 min and 80% for 5 min) and one bath of distilled water (5min). The samples were then sputter-coated with a thin layer of gold in an Edwards Sputter Coater, and observed with a Jeol JSM 6460LV scanning electron microscope.

3. Results and discussions

3.1. Microstructure

For each porosity content, SEM micrographs of the composite surface and cross section are shown in Figure 1. From the micrographs (Figure 1.a) to 1.d)), one can notice that the fibrous network is composed of curved fibre bundles, elementary fibres and a limited volume fraction of shives (4%). This type of composition is typical of raw materials coming from flax tows. Hence, shives will be ignored and the material will be assumed to be only reinforced by straight fibres in every direction, making the material quasi-isotropic in the horizontal plane. This assumption has been verified by tensile testing the composite in several directions.

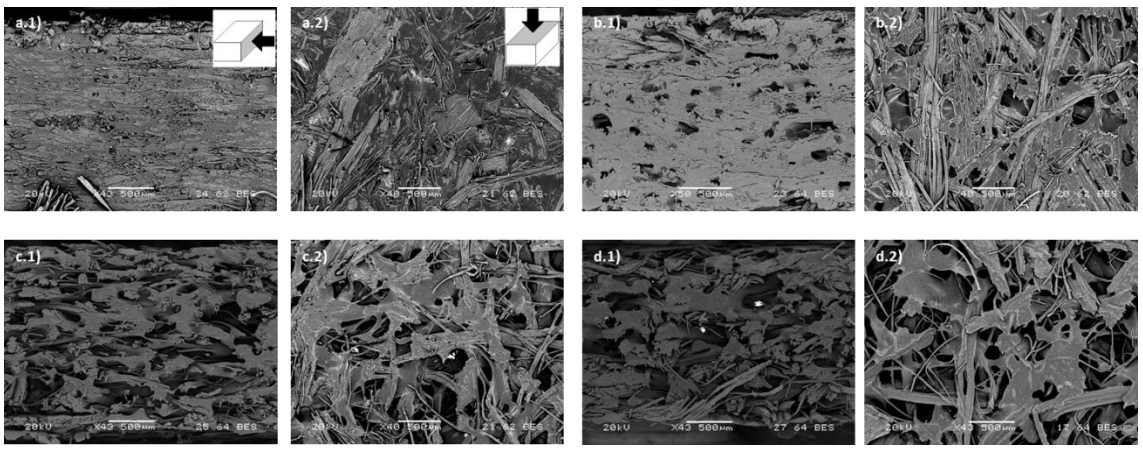

Figure 1. SEM micrographs of composite structure (a: Φ=5%, b: Φ =30%, c: Φ =60%, d: Φ =70%, 1: cross section, 2: surface)

Excerpt from ISBN 978-3-00-053387-7

Increasing the material compression rate corresponds to filling the fibrous network with an increasing quantity of matrix. At a 70% porosity content (Fig. 1.d)), porosities connect to each other through the plane, most of the fibres are dried but they are connected to others by matrix agglomerates like "glue dots" i.e. a small embedded fibre/matrix area. This structure is well known in the paper industry [14], where fibres are linked together by hydrogen bonds at their point of contact. At Φ=60% (Fig. 1.c)), the matrix starts embedding the fibres, however, the porosities still connect to each other through the plane. At Φ=30% (Fig 1.b)), porosities stop connecting to each other and impregnation porosity types (the matrix being unable to fill a gap between two fibres) are now observed [15]. Finally, at a low porosity level (Φ = 5%), only very small porosities are found and located at the fibre/matrix interface and in the matrix (Fig. 1.a)).
These observations highlight strong microstructural differences according to the composite porosity content which is related to processing parameters such as compaction rate.

3.2. Acoustic properties

Figure 2 shows the alpha coefficient measured at porosity contents of 5, 30, 60 and 70%. The measured values are similar to the literature on biocomposites made of nonwoven thermocompressed at different thicknesses [8].

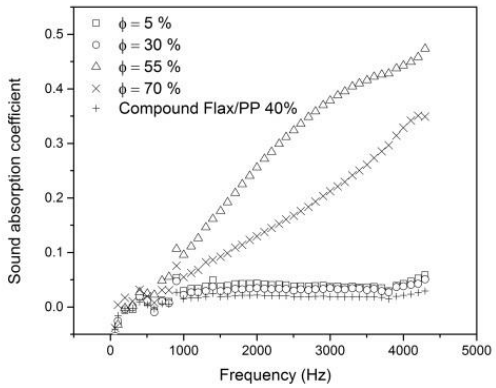

Figure 2. Normal sound absorption coefficients for biocomposites moulded at different porosity content and injected flax/PP compound as a function of sound wave frequency

From the results, it appears that the sound wave reflects on materials with limited porosity contents (5 and 30%) where pores are completely closed (Fig.1). This pore configuration creates a quasi-hermetic surface which leads to very low acoustic absorption ability [10]. When Φ=60%, the pores network is tortuous and crossed by dry fibres and composed of blind pores. The acoustic waves tend to disperse through the pore network and the dry fibres located into the pores tend to rub to each other and absorb energy [10]. Finally, increasing the porosity content enlarges and creates a network of percolating pores through the thickness. The damping capacity is then reduced.
The absorption coefficient of a reference material, i.e. a 40% vol. flax/PP compound, has also been characterized. Its absorption values are of the same order of magnitude than biocomposites obtained from nonwoven with limited porosity contents (5 and 30%) and having an hermetic surface. These poor acoustic performances are due to the fact that injected samples are injected with high compaction pressure, resulting in an almost 0% porosity material.
From this measurements, it appears that an optimum acoustic absorption coefficient is reached at Φ=60%. This highlights the necessity of creating tortuous porosity network by limiting the

Excerpt from ISBN 978-3-00-053387-7

compaction rate during process. However, the impact of this large porosity content on mechanical properties will have to be investigated.

3.3. Mechanical properties

3.3.1. Tensile behaviour and properties

Static tensile tests have been performed on composites moulded with different porosity contents ranging from 5 to 60% of the total volume. The tensile behaviour of each composite is presented in Figure 3.a). It is observed that a quick and complete rupture only occurs at low porosity content (Φ=5%). For higher porosity contents, once the maximal stress is reached, the composite keeps elongating with a low stress decrease. This behaviour is assumed to be typical of a progressive fibre network slippage. At Φ=60%, a point is reached where the bonds break quickly and the energy dissipation mechanisms could be the debonding of "glue dots" and fibre slippage (the composite keeps elongating with low stress decrease).
Prior to static tensile tests, the elasticity domain has been measured for each porosity content. The measured moduli (calculated on the elasticity domain) and maximal strength are shown in Figure 3.b). The porosity content has a strong influence on the tensile behaviour and properties of the composite, which is rather well fitted by a second order polynomial equation ($R^2 = 0.97$). This curve fitting helps to extrapolate the tensile modulus at 0% porosity content, which is within the same range than those found in the literature [6], [16], around 6100±1696 MPa.
The values of specific tensile properties of these biocomposites have been compared with literature data [17] obtained on flax/PP compounds at different fibre volume fraction (Fig. 3.c) and d)). From these plots, one can notice that it is more appropriate to choose material manufactured from nonwoven because they offer better strength and stiffness properties, even without using grafted PP. The range of properties obtained is also larger, bringing more flexibility in the material choice.

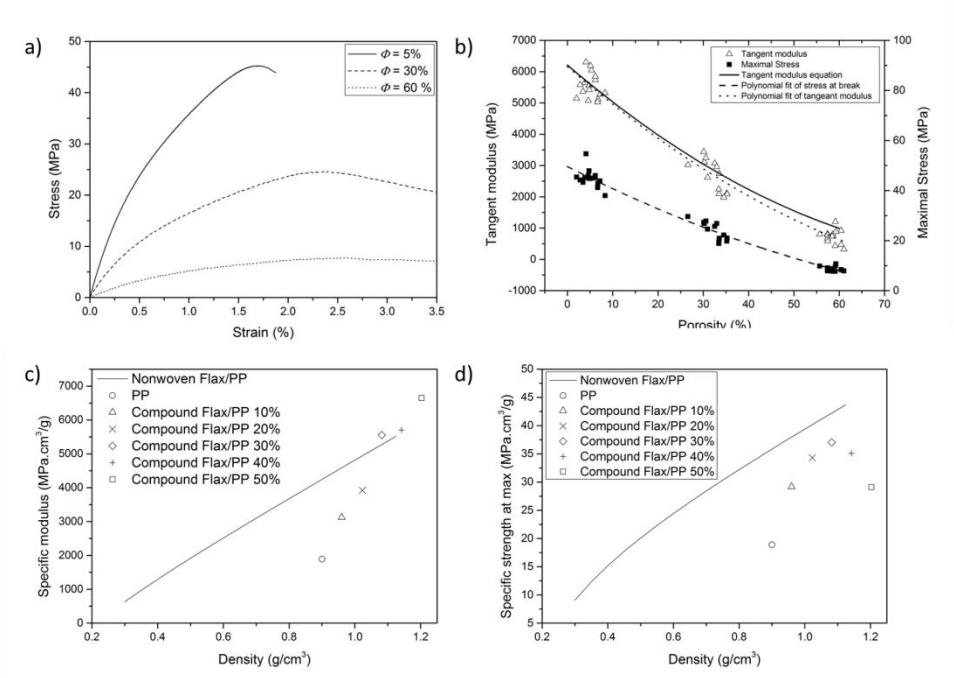

Figure 3. a) Tensile stress-strain behaviour according to porosity content. b) Young's modulus (triangular dots) and stress at break (squared dots) according to porosity content. Specific tensile modulus as a function of material density c) and strength d) for biocomposites moulded from nonwoven and compounds.

Excerpt from ISBN 978-3-00-053387-7

3.3.2. Assesment of damage mechanisms

To investigate composite damage mechanisms under stress, tensile tests under SEM with repeated progressive loading have been conducted. The damage variable *d* calculated with Equation 2 is plotted in Figure 4 as a function of normalized applied deformation $\varepsilon/\varepsilon_r$ where ε_r is the deformation at yield. For each porosity content, the damage plot is composed of two lines and its corresponding slope (s_a and s_b in the article) represents the damage progression while the load cycle is progressing.
At Φ=5% porosity, because of the relatively large matrix embedded length, rupture is mostly caused by the fibre, fibre bundle and matrix breakage but also by fibre/matrix debonding because of imperfect bonding. This type of failure has been previously observed by Rask et al on Flax/PP unidirectional composite [18]. For higher normalized deformation, post-debonding fibre/matrix friction due to thermal residual stress takes place after rupture and generates energy dissipation. These two behaviours are highlighted in Figure 4 by the presence of the slope 's_{a5}' representing debonding and breakage and the slope 's_{b5}' representing post debonding friction. The small difference between those two slope coefficients for Φ=5% is due to the higher contribution of friction to the interfacial bond strength in such systems (Flax/PP) rather than fibre/fibre interactions.
From 30% porosity contents, there is very little fibre breakage. Indeed, if the embedded length is lower than a critical value, fibre debonding occurs preferentially [19]. For these reasons, the *d* coefficient is assumed to mostly represent the behaviour of the interface bonding between fibre and matrix. At 30% porosity content (Fig. 4.2), a high damage rate during the first cycles is observed (first slope coefficient is s_{a30}=1.12). Cracks initiate perpendicularly to the tensile direction and propagate through connecting porosities. Once the interfacial bonds are broken, fibres are pulled out from the matrix. The contribution of post-debonding friction is weaker here than for Φ=5% due to the shorter gluing length, hence the energy dissipation by friction is lower (s_{b5} coefficient at Φ=5% is higher than at Φ=30%).
At Φ=60% (Fig. 4.3), the same behaviour is observed as before, however the damage values are lower due to lower initial modulus.
At 70% (Fig. 4.4), the transition between the rupture of the bonds and fibre slippage occurs quickly, reducing the difference between the two curves (s_{a70}=0.53 and s_{b70}=0.17). This low contribution of fibre/matrix adhesion is due to the very short fibre embedded length.
The deformation where the material switches from bond breaking to friction and fibre slippage decreases with the porosity level, from $\varepsilon/\varepsilon_r$=0.38 to 0.25. This value could describe the quality of the interface which is a combination of bond stress and embedded length.
When the porosity content increases, due to very low interfacial properties [20], the gluing surface parameter is the key to explain the overall mechanical properties and behaviour. Indeed, as suggested by Oksman, fibre tensile properties improvement will have a limited impact on the overall mechanical properties compared to fibre/matrix interface improvement [21].

Excerpt from ISBN 978-3-00-053387-7

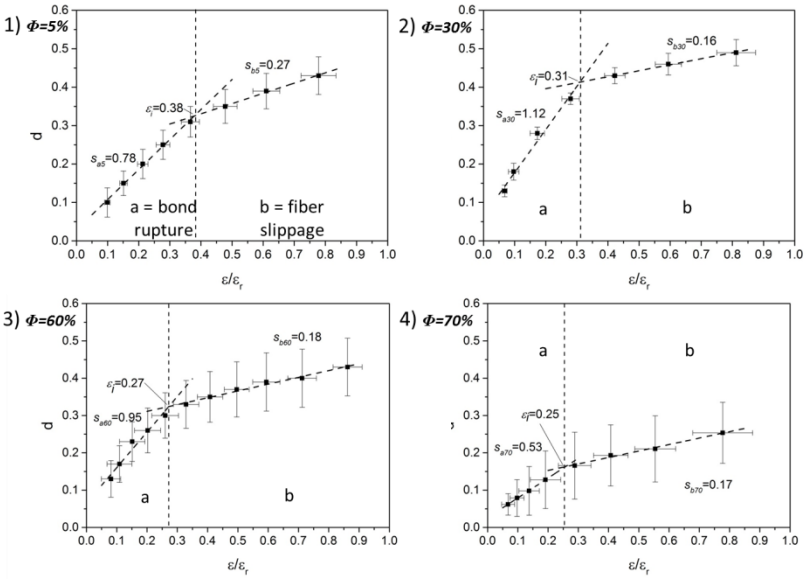

Figure 4. Damage variable as a function of normalized strain for different porosity contents

4. Conclusions

The nonwoven used in this study allows the part manufacturer to modify the material function (acoustic or mechanical) by changing the compaction rate during moulding. However, the influence of the porosity content on microstructural, acoustic and mechanical properties for a flax/PP nonwoven had to be assessed. A morphological analysis highlighted drastic changes of the composite microstructure according to the porosity level. Increasing the porosity content reduces the fibre/matrix embedded length and increases pore size up to a point where fibres are only connected to each other by glue dots and pores communicate through the entire thickness. As expected, this change of microstructure highly impacts the composite acoustic and mechanical behaviour. Moreover, repeated progressive loadings highlighted the presence of two damaging stages: fibre/matrix debonding and fibre slippage; the proportion of the two being governed by the embedded fibre length and the bond quality. The findings from this study could be extended to flexural and low impact velocity tests which are considered more realistic by automotive suppliers. The automotive industry is constantly looking for materials with good acoustic properties and reduced weight. This study shows how crucial it is to master the porosity level to optimize weight by offering a material with adjusted porosity content adapted to mechanical and acoustic requirements.

Acknowledgments

The authors would like to thank EcoTechnilin SAS® for supplying the fibres, the nonwoven materials and for funding this project. This project being part of the SINFONI program, the authors would also like to thank BPI France for their financial support.

References

[1] Alternative Fuel Vehicle Badging, Fuel Compartment Labels and Consumer Information on Alternative Fuel Usage, vol. 79. 2014.

[2] A. Bourmaud et C. Baley, « Investigations on the recycling of hemp and sisal fibre reinforced polypropylene composites », Polymer Degradation and Stability, vol. 92, n° 6, p. 1034‑1045, juin 2007.

Excerpt from ISBN 978-3-00-053387-7

[3] A. Lefeuvre, A. Bourmaud, C. Morvan, et C. Baley, « Tensile properties of elementary fibres of flax and glass: Analysis of reproducibility and scattering », Materials Letters, vol. 130, p. 289‑291, sept. 2014.
[4] S. Russell, Handbook of Nonwovens. Woodhead Publishing, 2006.
[5] H. Bos, J. Müssig, et M. Van den Oever, « Mechanical properties of short-flax-fibre reinforced compounds », Composites Part A: Applied Science and Manufacturing, vol. 37, no 10, p. 1591‑1604, oct. 2006.
[6] K. Oksman, « Mechanical Properties of Natural Fibre Mat Reinforced Thermoplastic », Applied Composite Materials, vol. 7, no 5‑6, p. 403‑414, nov. 2000.
[7] K.-P. Mieck, R. Lützkendorf, et T. Reussmann, « Needle-Punched Hybrid Nonwovens of Flax and PP Fibers-TextiIe Semi products for Manufacturing of Fiber Composites », Polymer Composites, vol. 17, no 6, p. 873‑878, déc. 1996.
[8] D. H. Mueller, A. Krobjilowski, H. Schachtschneider, J. Müssig, et G. Gescutti, « Acoustical properties of reinforced composite materials basing on natural fibers », présenté à Proceedings of the INTC-International Nonwovens Technical Conference, Atlanta, GA, 2002.
[9] A. Hao, H. Zhao, et J. Y. Chen, « Kenaf/polypropylene nonwoven composites: The influence of manufacturing conditions on mechanical, thermal, and acoustical performance », Composites Part B: Engineering, vol. 54, p. 44‑51, nov. 2013.
[10] M. J. Crocker, Handbook of Noise and Vibration Control. John Wiley & Sons, 2007.
[11] B. Madsen, A. Thygesen, et H. Lilholt, « Plant fibre composites – porosity and stiffness », Composites Science and Technology, vol. 69, no 7‑8, p. 1057‑1069, juin 2009.
[12] B. Madsen et H. Lilholt, « Physical and mechanical properties of unidirectional plant fibre composites—an evaluation of the influence of porosity », Composites Science and Technology, vol. 63, no 9, p. 1265‑1272, juill. 2003.
[13] P. Davies, F. MazÉas, et P. Casari, « Sea Water Aging of Glass Reinforced Composites: Shear Behaviour and Damage Modelling », Journal of Composite Materials, vol. 35, no 15, p. 1343‑1372, janv. 2001.
[14] K. Niskanen, Mechanics of Paper Products. Walter de Gruyter, 2011.
[15] B. Madsen, A. Thygesen, et H. Lilholt, « Plant fibre composites – porosity and volumetric interaction », Composites Science and Technology, vol. 67, no 7‑8, p. 1584‑1600, juin 2007.
[16] S. K. Garkhail, R. W. H. Heijenrath, et T. Peijs, « Mechanical Properties of Natural-Fibre-Mat-Reinforced Thermoplastics based on Flax Fibres and Polypropylene », Applied Composite Materials, vol. 7, no 5‑6, p. 351‑372, nov. 2000.
[17] G. Ausias, A. Bourmaud, G. Coroller, et C. Baley, « Study of the fibre morphology stability in polypropylene-flax composites », Polymer Degradation and Stability, vol. 98, no 6, p. 1216‑1224, juin 2013.
[18] M. Rask, B. Madsen, B. F. Sørensen, J. L. Fife, K. Martyniuk, et E. M. Lauridsen, « In situ observations of microscale damage evolution in unidirectional natural fibre composites », Composites Part A: Applied Science and Manufacturing, vol. 43, no 10, p. 1639‑1649, oct. 2012.
[19] B. Miller, P. Muri, et L. Rebenfeld, « A microbond method for determination of the shear strength of a fiber/resin interface », Composites Science and Technology, vol. 28, no 1, p. 17‑32, 1987.
[20] N. Graupner, J. Rößler, G. Ziegmann, et J. Müssig, « Fibre/matrix adhesion of cellulose fibres in PLA, PP and MAPP: A critical review of pull-out test, microbond test and single fibre fragmentation test results », Composites Part A: Applied Science and Manufacturing, vol. 63, p. 133‑148, août 2014.
[21] K. Oksman, A. P. Mathew, R. Långström, B. Nyström, et K. Joseph, « The influence of fibre microstructure on fibre breakage and mechanical properties of natural fibre reinforced polypropylene », Composites Science and Technology, vol. 69, no 11‑12, p. 1847‑1853, sept. 2009.

Excerpt from ISBN 978-3-00-053387-7